MODELING, SIMULATION, PROTOTYPING & VALIDATION

Assessment of Artificial Magnetic Conductor Checkerboard-Arranged Applique for Ground System Radar Cross Section Reduction

Nathan Tison
Jeffrey D'Archangel

Background and Motivation

- Simply put, radar cross section (RCS) is basically a measure of materiel detectability by threat radar, and is therefore something we would generally want to reduce.
- An advantageous means of RCS reduction (RCSR) would involve: (1) redirecting the reflected radar energy away from the receiver; (2) broadband performance; (3) no significant change to the materiel geometry; (4) the use of only a thin / light structure / applique; and (5) passive operation.
- One potential way to accomplish all of these goals would involve the use of a two-dimensional metamaterial (or metasurface).
- A type of metasurface which can be used could consist of artificial magnetic conductors (AMCs) composed of a ground plane, a dielectric substrate, and a metallic patch pattern.
- The benefit of these AMCs is that they involve reflection phases which vary “continuously from +180^{o} to -180^{o} as the frequency increases” [1] through some resonant condition.
- Two different AMCs could be selected and configured in a square checkerboard pattern for purposes of maximizing the destructive interference of the radar energy reflected in the specular direction over as broad a bandwidth as possible, with the single, large, specular reflection lobe being exchanged for four, small, non-specular reflection lobes [3].
- A relatively thin AMC checkerboard-arranged applique (ACA) could be constructed and adhered to materiel surfaces for RCSR purposes.

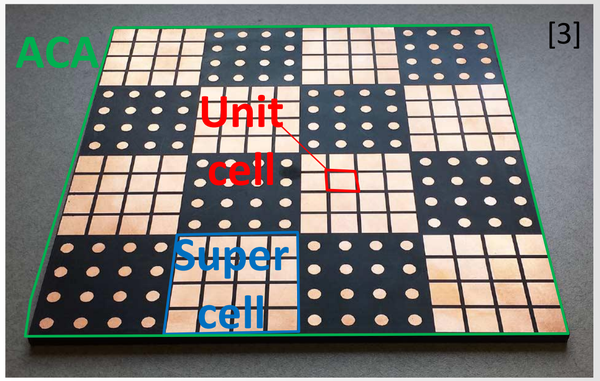

[3]

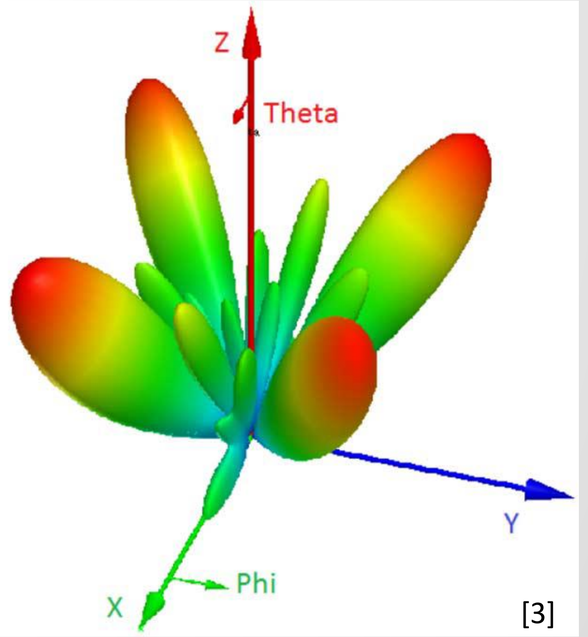

[3]

Objectives

The main goals of this study included:

1. The development of an efficient methodology for identifying / designing an ACA concept which satisfies RCSR performance requirements and other constraints.
2. The development of both simpler lumped-parameter models (LPM) and more computationally-intensive high-fidelity models (HFM) of ACA concept performance, and model validation using literature data.
3. The general performance assessment of the most promising ACA concept, including RCS assessment of a notional vehicle with and without the integrated ACA concept using a medium-fidelity model (MFM), which would also be validated.

RCSR Performance Requirement Development

In order to have a standard against which the performance of the developed ACA concepts could be assessed, an RCSR performance requirement was developed:

"The applique should provide an average RCSR relative to a perfect electrical conductor (PEC) surface – from L- to X-band, for both transverse electric field (TE) and transverse magnetic field (TM) polarizations, and for normal incidence – which is greater than 10dB over at least 50% of the bandwidth, and is characterized by a bandwidth-averaged return elevation angle delta (with respect to normal incidence) which is as close to 45 degrees as possible."

AMC Geometry Selection

Rectangular Patch

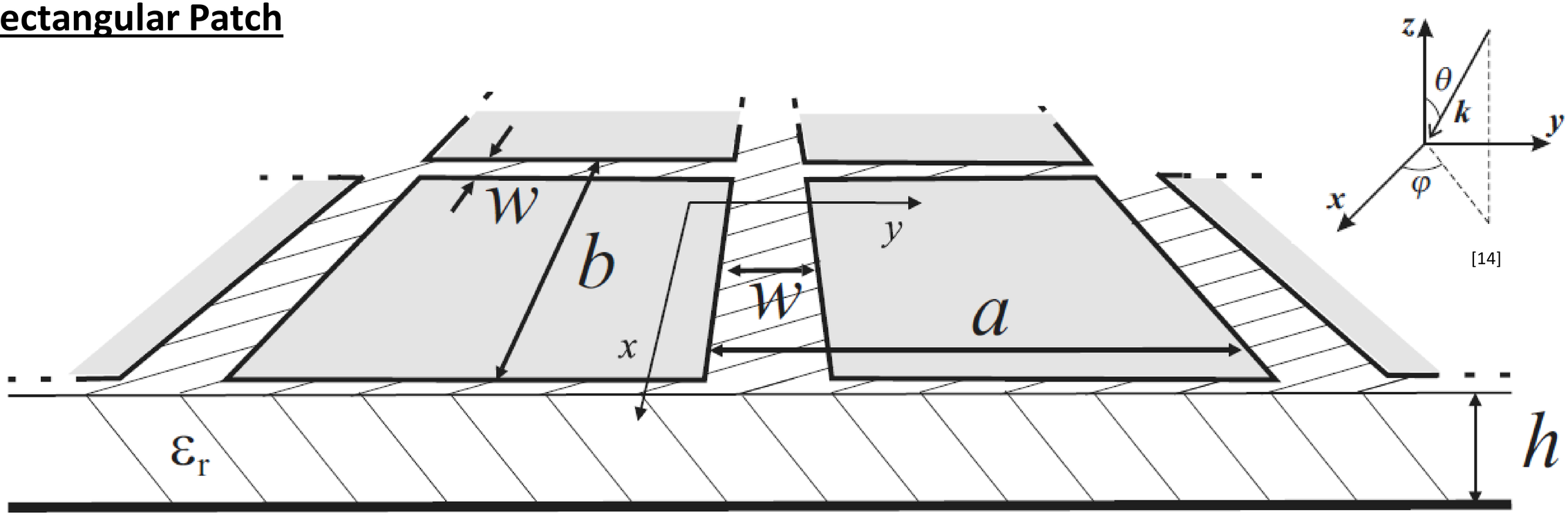

[14]

A rectangular-patch metallic pattern was selected due to its simplicity, its ease of fabrication and suitability for use in ACAs, and the availability of LPM performance relations (which allow for full variation of the electromagnetic incidence angles for both polarizations) as well as HFM performance results (within the literature).

AMC LPM Development

Impedance Prediction Capability

So the first step is to develop predictive capability for the ACA "building blocks" – the AMCs. We start here with the LPM (of the impedance).

- **Impedance**

The AMC impedance Z was determined using transmission line theory [14] as follows:

$$Z_i^{TM} = \frac{j\omega\mu_0\mu_r\frac{\tan(\beta h)}{\beta}\zeta}{1-2k_{eff}\alpha_{TM}\frac{\tan(\beta h)}{\beta}\zeta} \qquad Z_i^{TE} = \frac{j\omega\mu_0\mu_r\frac{\tan(\beta h)}{\beta}}{1-2k_{eff}\alpha_{TE}\frac{\tan(\beta h)}{\beta}\xi}$$

where ω is the angular frequency,

$k = k_0\sqrt{\varepsilon_r}$,

$k_t = k_0 \sin\theta_0$ [8],

$\varepsilon_{eff} = \frac{\varepsilon_r+1}{2}$,

$\alpha_{TM} = \frac{k_{eff}a_{TM}}{\pi}\ln\left(\frac{1}{\sin\frac{\pi w}{2a_{TM}}}\right)$, $\alpha_{TE} = \frac{k_{eff}a_{TE}}{\pi}\ln\left(\frac{1}{\sin\frac{\pi w}{2a_{TE}}}\right)$,

$\theta_2 = \frac{\arcsin(\sin\theta_0)}{\sqrt{\varepsilon_r}}$,

$\xi = 1 - \frac{a_{TM}}{a_{TM}+a_{TE}}\left(\frac{k_0 \sin\theta_0}{k_{eff}}\right)^2$

$\beta = \sqrt{k^2 - k_t^2}$,

k_0 is the free-space wave number,

$k_{eff} = k_0\sqrt{\varepsilon_{eff}\mu_{eff}}$,

$\mu_{eff} = \frac{\mu_r+1}{2}$,

$\zeta = \cos^2\theta_2$,

Frequency-Independent Input and Intermediate Data		
Type	**Parameter ***	**Units**
Inputs	Dielectric real relative permittivity ε_r'	-
	Dielectric loss tangent δ	
	Dielectric relative permittivity ε_r	
	Dielectric relative permeability μ_r	
	Free space permittivity ε_0	F/m
	Free space permeability μ_0	H/m
	Incidence elevation angle θ_0	deg
	Incidence azimuth angle ϕ_0	
	Dielectric thickness h	m
	Supercell periodicity d_{TM} within TM POI	
	Supercell periodicity d_{TE} within TE POI	
	AMC patch gap w	
	Minimum number of unit cells along TM POI	-
	Minimum number of unit cells along TE POI	
	RCSR goal	dB
Intermediates	AMC periodicity a_{TM} within TM POI	m
	AMC periodicity a_{TE} within TE POI	
	Free space impedance for TM polarization η_0^{TM}	Ω
	Free space impedance for TE polarization η_0^{TE}	
	Effective relative permittivity ε_{eff}	-
	Effective relative permeability μ_{eff}	
	Refraction angle θ_2	deg

* "TM" denotes transverse magnetic polarization, "TE" denotes transverse electric polarization, "POI" denotes plane of incidence

AMC LPM Development

Reflection Prediction Capability

- **Reflection Phase**

  The supercell reflection phase P for AMC "i" and polarization "j" with respect to free-space impedance Z_0 can be expressed as [4]:

$$P_i^j = \mathrm{Im}\left[\ln\left(\frac{Z_i^j - Z_0^j}{Z_i^j + Z_0^j}\right)\right]$$

  where for free space

$$Z_0^{TM} = \eta_0 \cos\theta_0$$

  and

$$Z_0^{TE} = \frac{\eta_0}{\cos\theta_0}$$

- **Reflection Amplitude**

  The supercell reflection amplitude A can be expressed as:

$$A_i^j = \left|\frac{Z_i^j - Z_0^j}{Z_i^j + Z_0^j}\right|$$

- **Reflection Loss**

  The supercell reflection loss RL (in dB) can be expressed as:

$$RL_i^j = -20 \log A_i^j$$

AMC HFM Development

- A numerical, high-fidelity modeling (HFM) approach for simulating the AMC supercell was developed using the COMSOL 5.6 RF module [15].
- This approach uses the finite element method to compute the amplitude and phase of reflected waves from electromagnetic structures.
- It employs the Floquet port method, which …
  - Allows simulation of a supercell by considering only a single unit cell.
  - Correctly accounts for phase shifts due to angle of incidence.
  - Simulates spectral properties in terms of scattering (S) parameters.

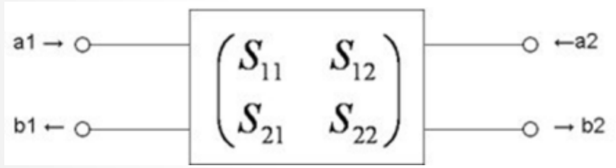

$$\begin{bmatrix} b_1 \\ b_2 \end{bmatrix} = \begin{bmatrix} S_{11} & S_{12} \\ S_{21} & S_{22} \end{bmatrix} \begin{bmatrix} a_1 \\ a_2 \end{bmatrix}$$

$$R = |S_{11}|^2 \;;\; T = |S_{21}|^2$$

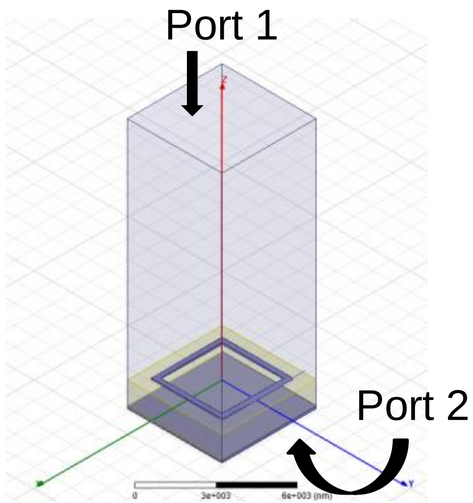

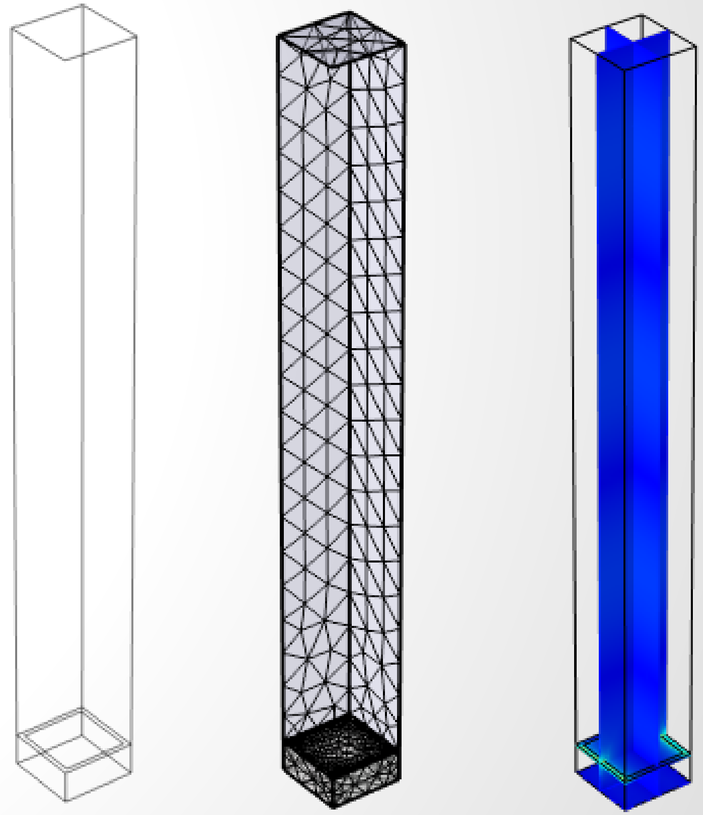

AMC LPM / HFM Validation

Square patch AMC results from the literature [1] are used to validate both the LPM and HFM approaches for the square patch geometry of the unit cell shown to the right.

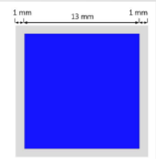

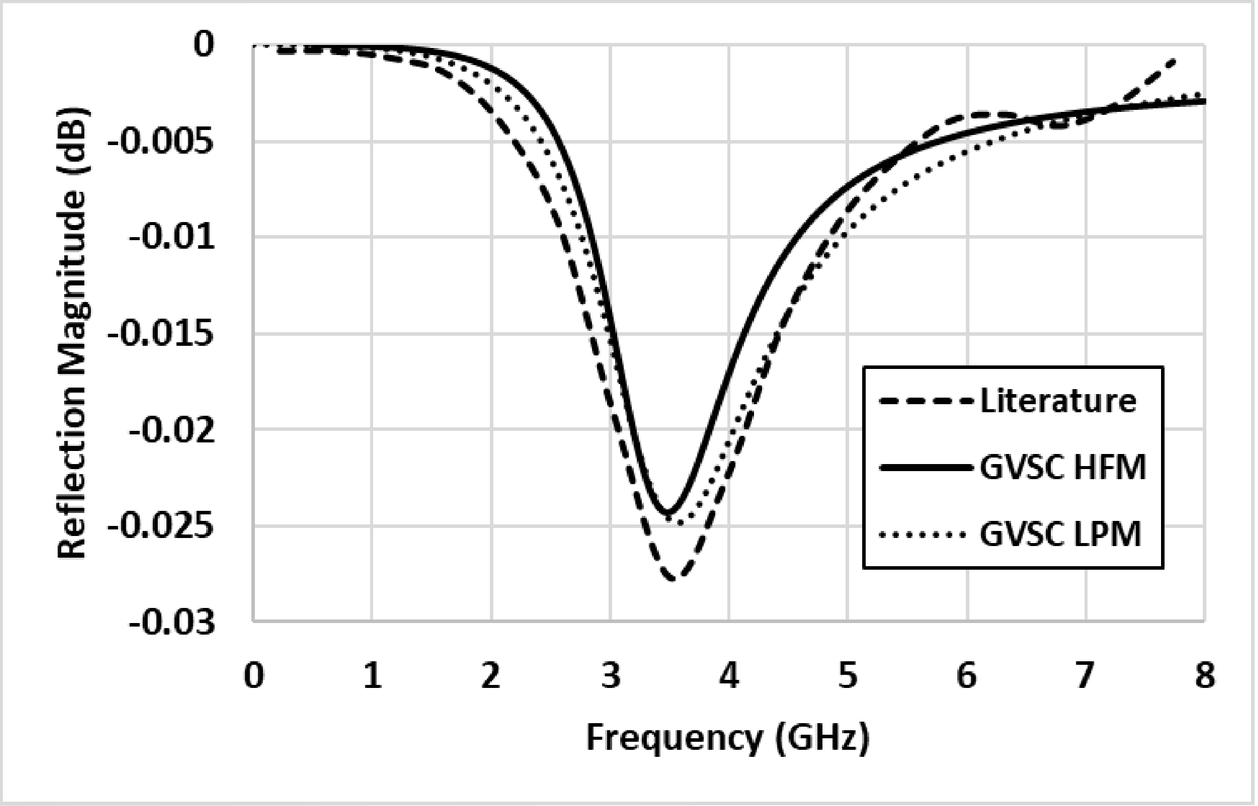

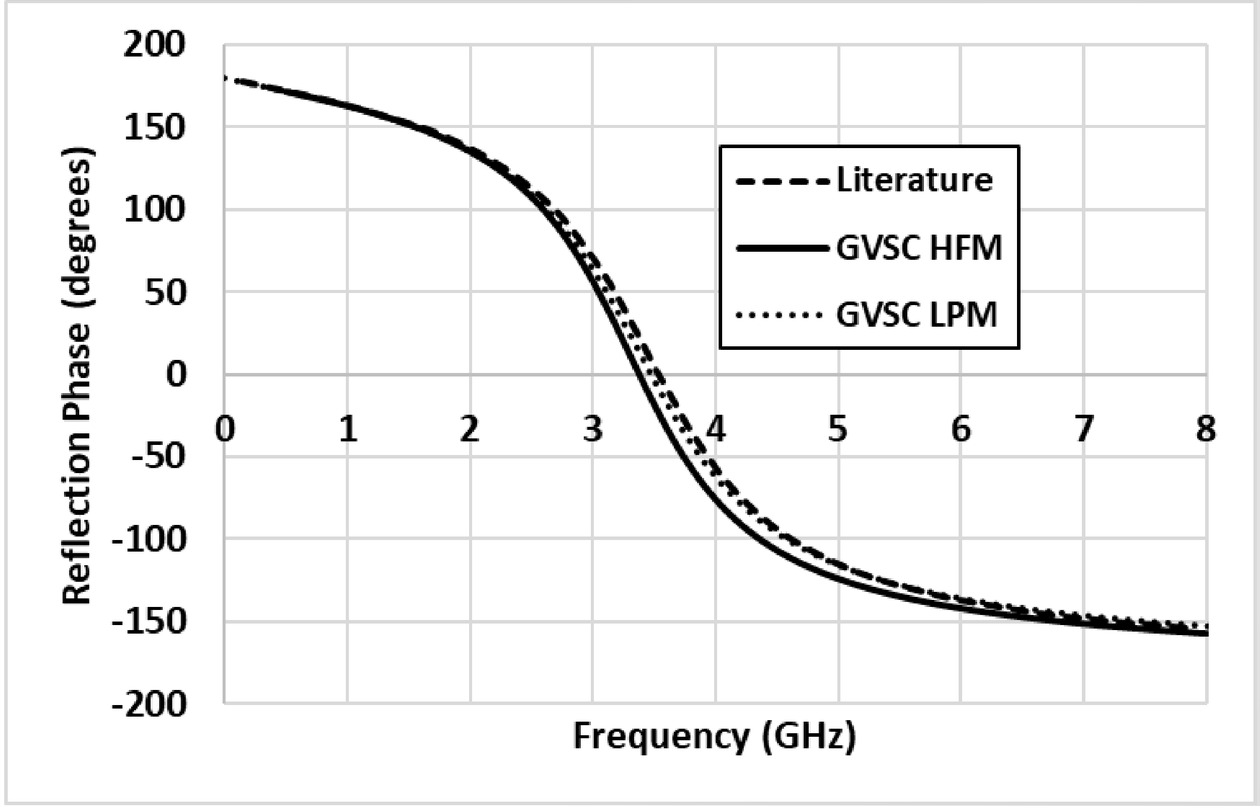

Good agreement among the LPM, HFM, and literature results for the amplitude and phase characteristics of square patch reflection can be observed.

ACA LPM Development

Scattered Lobe Direction and RCSR Predictive Capability

- **Scattered Lobe Direction**

  Using antenna planar array theory, the direction of the supercell scattering (grating) lobes can be approximately determined using the following expressions [12]:

Up until now, the focus has been on the AMC model development. Now, we turn our attention to the ACA model development.

$$\tan\phi^{j}_{m,n} = \frac{\sin\theta_0 \sin\phi_0 \pm (2n+1)\frac{\Delta P^{j}_{TM}}{kd_{TM}}}{\sin\theta_0 \cos\phi_0 \pm (2m+1)\frac{\Delta P^{j}_{TE}}{kd_{TE}}}$$

$$\sin^2\theta^{j}_{m,n} = \left[\sin\theta_0 \sin\phi_0 \pm (2n+1)\frac{\Delta P^{j}_{TM}}{kd_{TM}}\right]^2 + \left[\sin\theta_0 \cos\phi_0 \pm (2m+1)\frac{\Delta P^{j}_{TE}}{kd_{TE}}\right]^2$$

where θ and ϕ denote the elevation and azimuth angles with respect to the surface normal direction, 0 the incidence angles, ΔP the supercell phase shift, k the substrate wave number, d the supercell size, TE and TM the surface-tangential directions aligned with the TE and TM planes of incidence respectively, and m and n the reflection grating lobe order. The four major lobes can be determined by allowing m and n to equal zero [3].

- **RCSR**

  A relation for ACA RCSR relative to a PEC is [1]:

$$\mathrm{RCSR} = 10\log\left[\frac{A_1 e^{jP_1} + A_2 e^{jP_2}}{2}\right]^2$$

where "A" denotes the reflection amplitude, "P" denotes the reflection phase, and the numeric subscript identifies the AMC supercell type.

ACA LPM Development

Fresnel Coefficient Predictive Capability

- **Fresnel <u>Reflection</u> Coefficients**
  - For <u>Transverse Electrical</u> Polarization [5]

$$R_{TE} = \frac{Z_i^{TE} - Z_0^{TE}}{Z_i^{TE} + Z_0^{TE}}$$

  - For <u>Transverse Magnetic</u> Polarization [5]

$$R_{TM} = \frac{Z_i^{TM} - Z_0^{TM}}{Z_i^{TM} + Z_0^{TM}}$$

- **Fresnel <u>Transmission</u> Coefficients**

  While the relations for normal materials could generally be expressed for TE polarization and TM polarization [5], the ground planes of these AMCs do not allow the development of an electric field and thereby prevent propagation of essentially any energy through the material. Therefore, for these AMCs, it can be effectively stated that …

  - For <u>Transverse Electrical</u> Polarization

$$T_{TE} = 0$$

  - For <u>Transverse Magnetic</u> Polarization

$$T_{TM} = 0$$

Now that we've developed the ACA LPM, we can use it to perform optimization studies.

ACA LPM Optimization Study

General Approach

- **Parameters Varied:**
  - Dielectric relative permittivity magnitude.
  - Dielectric relative permittivity loss tangent.
  - Dielectric thickness.
  - Supercell periodicity. Since best results were obtained for equal periodicities along both directions, they were set equal.
  - Patch gaps for AMCs 1 and 2.

Note: Regarding the number of unit cells (per supercell). It was determined that minimizing the number of unit cells maximizes the scattering lobe elevation angles and azimuth angle standard deviations (both beneficial). However, it was also determined that the minimum number of unit cells which still allow supercell AMC behavior to be obtained is four [10]. Therefore, four unit cells were used.

- **Scenarios Considered:**
  Incident elevation angle of only 0 degrees, since it did not seem to be a significant discriminator of candidate performance.

- **Metrics Used:**
  - **Primary:**
    - BWF meeting RCSR goal
    - RCSR
  - **Secondary:**
    - Scattering lobe elevation angle delta
    - Scattering lobe azimuth angle standard deviation

- **Methods Employed:**
  - **Manual Approach:** Involves "trial-and-error" selection of parameters to best improve the RCSR performance.
  - **DOE Approach:** Involves a more systematic exploration technique to best improve the RCSR performance.
    - **Generation of the DOE studies:** Latin hypercube sampling was used to generate a large number of simulation cases, involving as wide a variation of the input parameters as possible. A MATLAB script was used for this purpose.
    - **Execution of the DOE studies:** A Visual Basic script was used within the Excel-based LPM to solve several hundred thousands of cases. Multiple studies were performed, with the input parameter ranges becoming increasingly narrow, based upon the emerging results, for purposes of honing in on the best-performing case.

ACA LPM Optimization Study

Results

MODELING, SIMULATION, PROTOTYPING & VALIDATION

Tabulated Data

Input Data					
Description	Units	Value			
		Manually-Optimized		DOE-Optimized	
		AMC 1	AMC 2	AMC 1	AMC 2
Dielectric relative permittivity magnitude	-	2.200		2.401	
Dielectric permittivity loss tangent		0.010		0.066	
Dielectric thickness	mm	6.50		3.78	
Unit cell periodicity		25.00		15.69	
AMC patch gap		4.90	22.40	2.65	13.62

Output Data			
Description *	Units	Value	
		Manually-Optimized	DOE-Optimized
Bandwidth fraction meeting RCSR goal	%	43.1	64.6
RCS reduction	dB	8.56	10.72
Scattering lobe elevation angle delta	deg	15.5	21.2
Scattering lobe azimuth angle standard deviation		45.0	45.0

* Outputs are band-averaged with the exception of the bandwidth fractions

Graphical Data

Manually-"Optimized"

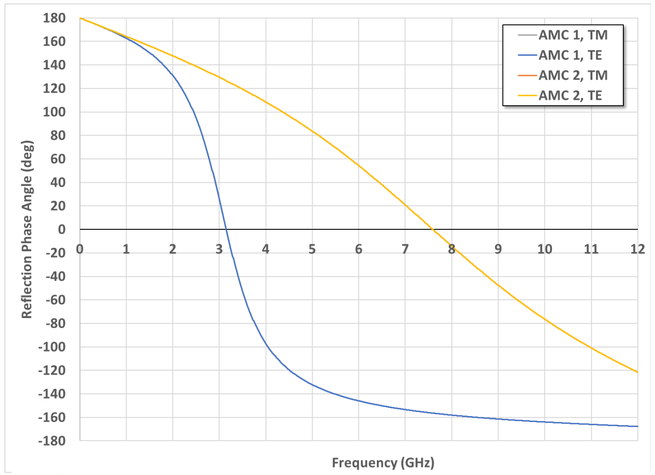

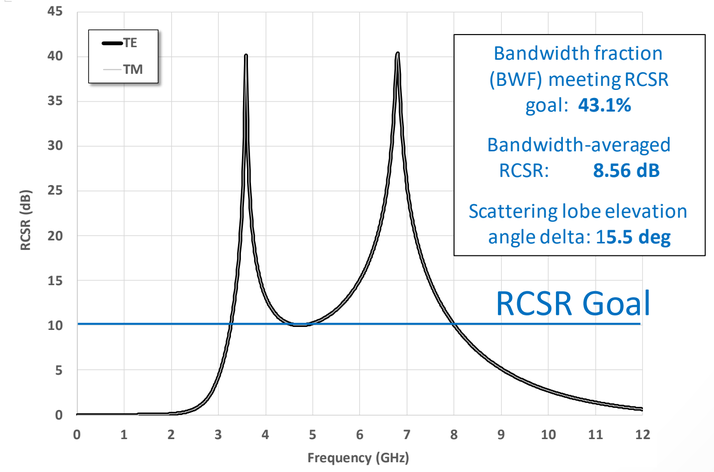

DOE-Optimized

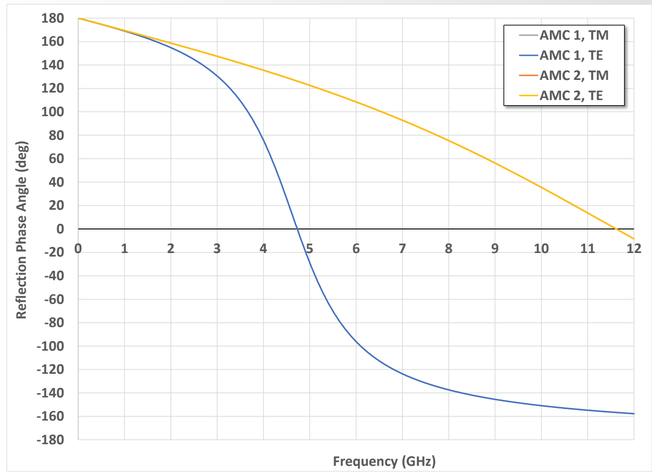

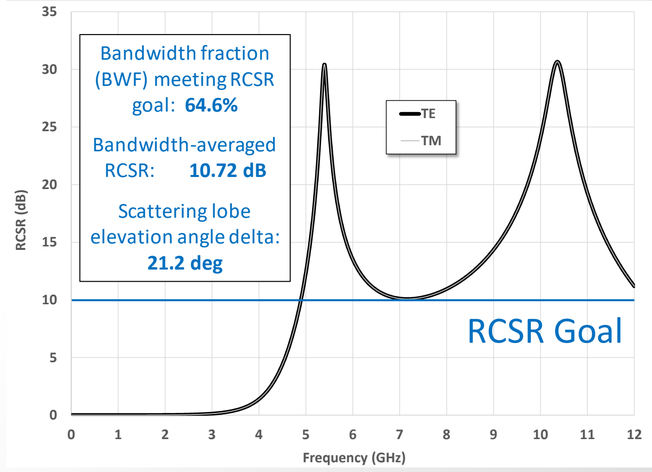

The DOE-optimized ACM pairing performs significantly better than the manually-optimized ACM pairing.

ACA MFM Development

- What's ultimately needed is ACA performance predictive capability which can accommodate realistic vehicle integration geometries.
- A review of the ACA predictive capability developed so far reveals that …
  - The LPM only accommodates simple, flat-plate scenarios.
  - The HFM cannot accommodate complex geometries due to its solving of the full Maxwell equations.
- To fill this gap, it would be desirable to develop "in-between" (or MFM) predictive capability, which would involve the solution of the governing Maxwell equations which are simplified for the optical regime using the Xpatch computational electromagnetics asymptotic solver.
- Xpatch uses the shooting and bouncing ray (SBR) tracing method, combining geometric and physical optics methods. Diffraction effects are modeled based upon the physical theory of diffraction. Material discontinuities and both co- and cross-polarizations are accounted for.
- The MFM would be used to model the ACAs and predict the interactions of the checkerboard-patterned AMC supercells.
- The MFM is developed based upon the following considerations / assumptions:
  - Bare vehicle surfaces can be modeled as PEC.
  - The AMC supercells can be modeled using Fresnel reflection and transmission coefficients. These coefficients – involving both the real and imaginary components for both the TE and TM polarizations – were determined for the DOE-optimized AMC supercell combination over the full range of frequencies and incidence angles using a Visual Basic script.

ACA MFM Plate Study

Methodology

- Using the MFM, a simple flat plate analysis was performed for purposes of comparing a “bare plate” and an “ACA-treated plate”.
- “AMC 1” is shown in red color, while “AMC 2” is shown in blue color.
- The angle of incidence is assumed to vary only in the azimuth (and not elevation) direction.
- For purposes of simplicity, the results associated with only the two co-polarizations – vertical receive / transmit (VV) and horizontal receive / transmit (HH) – are considered.
  - Rationale: Co-polarization returns are generally more significant than cross-polarization returns.
  - Note: The VV polarization results are associated with the TE-polarization AMC behavior, and the HH polarization results are associated with the TM-polarization AMC behavior.

ACA-Treated Plate

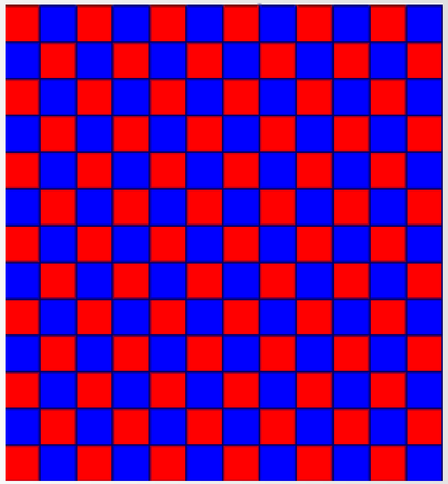

Bare Plate

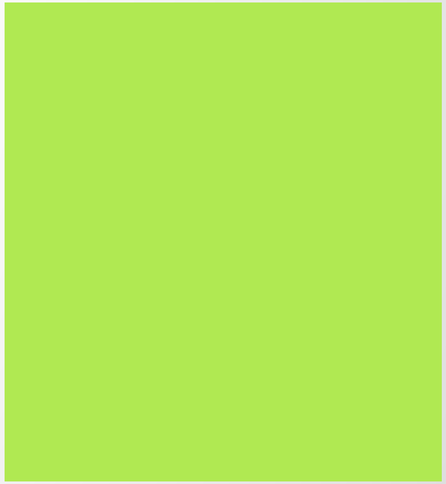

ACA MFM Plate Study

Results

RCSR | **BWF**

VV

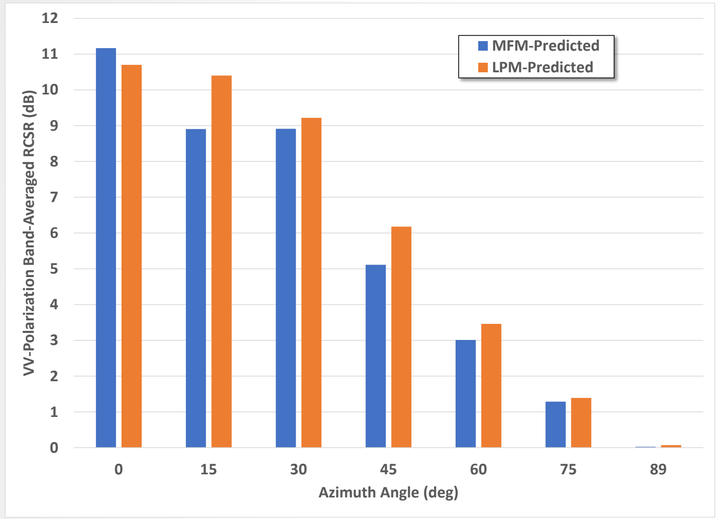

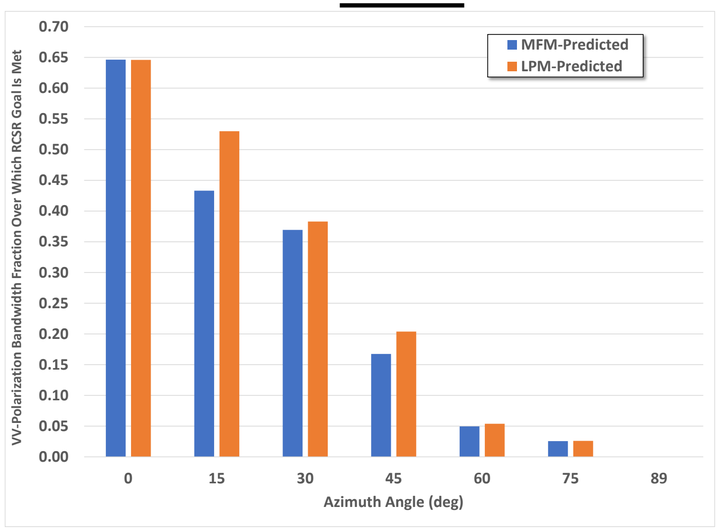

HH

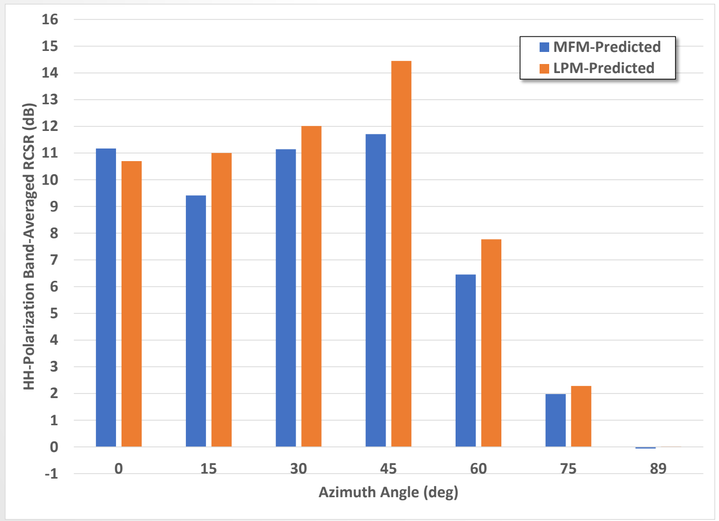

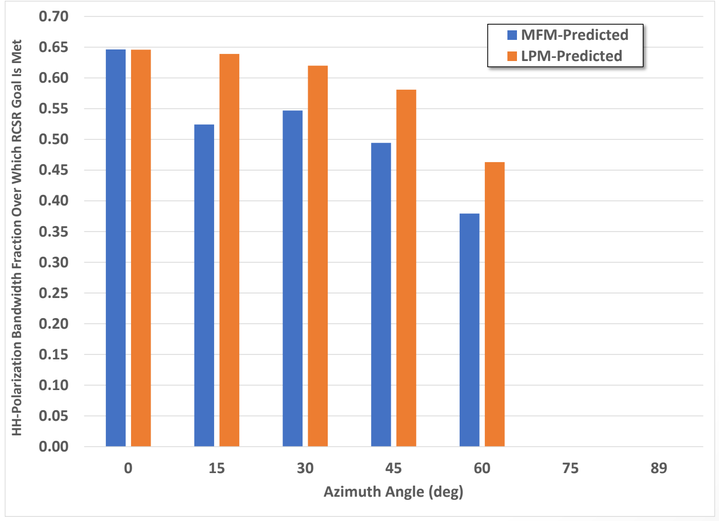

The MFM plate study results – including both the predicted RCSR and BWF over which the RCSR goal is met – compare relatively favorably with the LPM results, especially at normal (zero degrees) incidence angle, which is the most important incidence angle as it relates to RCSR.

Summary / Conclusions

- It was desired to develop a thin ACA metasurface concept which could be constructed and adhered to materiel surfaces for purposes of reducing radar signature.
- A rectangular-patch metallic pattern was selected due to its simplicity, ease of fabrication, and availability of both LPM performance relations and HFM performance results in the literature for validation purposes; however, the lack of consideration of other topologies limited RCSR performance potential.
- A notional RCSR performance requirement was developed for the purpose of having a means by which to compare and evaluate the developed concepts.
- AMC LPMs and HFMs were successfully developed and validated using experimental data from the literature.
- ACA LPMs and MFMs were successfully developed and correlated.
- Using the ACA LPM, the DOE-optimized ACM pairing was found to perform significantly better than the manually-optimized ACM pairing.
- Using the ACA MFM, an MFM plate study was performed in which RCSR and BWF results were shown to compare relatively favorably with the LPM results, especially at normal (zero degrees) incidence angle, which is the most important incidence angle as it relates to RCSR.
- Additional integration studies were performed, and may be presented in the future.
- For the purpose of developing an ACA concept synthesis and optimization approach, GP approaches, methodologies, and tools were researched and considered, and a GP-based plan for follow-on efforts was established at a high level; however, due to resource constraints, an alternative FNN surrogate modeling approach was initiated instead.

References

[1] Chen, Wengang, Constantine A. Balanis, and Craig R. Birtcher. "Checkerboard EBG surfaces for wideband radar cross section reduction." IEEE Transactions on Antennas and Propagation 63.6 (2015): 2636-2645.

[2] Rayno, Jennifer H. Development and application of genetic programming in the design and optimization of ultra-wideband 3D metamaterials. Diss. Univ. of Hawai'i at Manoa, 2016.

[3] Balanis, Constantine A., et al. "Applications of AMC-based impedance surfaces." EPJ Applied Metamaterials 5 (2018): 3.

[4] Sievenpiper, Daniel Frederic. High-impedance electromagnetic surfaces. University of California, Los Angeles, 1999.

[5] Balanis, Constantine A. Advanced engineering electromagnetics. John Wiley & Sons, 2012.

[6] Luukkonen, Olli, et al. "Simple and accurate analytical model of planar grids and high-impedance surfaces comprising metal strips or patches." IEEE Transactions on Antennas and Propagation 56.6 (2008): 1624-1632.

[7] Xu, Yuan, and Mang He. "Design of multilayer frequency-selective surfaces by equivalent circuit method and basic building blocks." International Journal of Antennas and propagation 2019 (2019).

[8] Costa, Filippo, Agostino Monorchio, and Giuliano Manara. "An overview of equivalent circuit modeling techniques of frequency selective surfaces and metasurfaces." The Applied Computational Electromagnetics Society Journal (ACES) (2014): 960-976.

[9] Hosseinipanah, Mirshahram, and Qun Wu. "Equivalent circuit model for designing of Jerusalem cross-based artificial magnetic conductors." Radioengineering 18.4 (2009): 544-550.

[10] Galarregui, Juan Carlos Iriarte, et al. "Broadband radar cross-section reduction using AMC technology." IEEE Transactions on Antennas and Propagation 61.12 (2013): 6136-6143.

[11] Durgun, Ahmet Cemal. Analysis, Design, Simulation, and Measurements of Flexible High Impedance Surfaces. Arizona State University, 2013.

[12] Balanis, Constantine A., et al. "Applications of AMC-based impedance surfaces." EPJ Applied Metamaterials 5 (2018): 3.

[13] Sang, Di, et al. "Design of checkerboard AMC structure for wideband RCS reduction." IEEE Transactions on Antennas and Propagation 67.4 (2019): 2604-2612.

[14] O. Luukkonen, “Artificial impedance surfaces,” Ph.D. Dissertation, Department of Radio Science and Engineering,

Helsinki University of Technology, Espoo, Finland, 2009.

[15] COMSOL v. 5.6 RF module user manual.